Phonon renormalization at small q values in the high-temperature phase of $CsCuCl_3$

1997 J. Phys.: Condens. Matter 9 1067

(http://iopscience.iop.org/0953-8984/9/5/012)

J. Phys.: Condens. Matter **9** (1997) 1067–1077. Printed in the UK PII: S0953-8984(97)74999-3

Phonon renormalization at small q values in the high-temperature phase of $CsCuCl_3$

U Förster, H A Graf, U Schotte and U Stuhr
Hahn-Meitner-Institut, Berlin, Germany

Received 31 May 1996, in final form 31 October 1996

Abstract. The hexagonal perovskite $CsCuCl_3$ exhibits a structural phase transition from a dynamically disordered high-temperature phase to an ordered low-temperature phase due to the cooperative Jahn–Teller effect. The lattice dynamics of the high-temperature phase has been studied by inelastic neutron scattering experiments. The investigations concentrated on small wave vectors q, where for the first time renormalized phonons at $q = 0.02$–0.05 Å^{-1} could be observed. The measurements confirm the predictions of a theoretical approach based on the coupling between dynamic reorientation processes and acoustic lattice waves (pseudo-spin phonon coupling).

1. Introduction

$CsCuCl_3$ belongs to a group of cooperative Jahn–Teller systems $AMCl_3$ ($A = Rb^+$, Cs^+; $M = Cu^{2+}$, Cr^{2+} as Jahn–Teller active ions), which have been studied extensively in the past [1–7]. Their structures are closely related to the hexagonal perovskite type with chains of face-sharing MCl_6 octahedra extending along the crystallographic c axis. All these compounds have a disordered high-temperature phase of apparent high symmetry described by the space group $P6_3/mmc$ (see figure 1). They undergo one (Cs compounds) or two (Rb compounds) structural phase transitions. $CsCuCl_3$ exhibits a first-order phase transition leading to an ordered low-temperature phase. When approaching the phase transition from below by heating the sample it was always found to occur at 423 K. A large hysteresis, however, is observed, when cooling the sample. Here the phase transition usually takes place between 418 and 410 K, depending on the crystal volume and quality. In contrast to all the other compounds, which finally become monoclinic, the ordered phase of $CsCuCl_3$ remains hexagonal with space group $P6_122$ and the c axis tripled. Due to the Jahn–Teller effect the $CuCl_6$ octahedra are distorted. They are tetragonally elongated (octahedra of approximately tetragonal symmetry with axes $d_1 = 5.52$ Å and $d_2 = d_3 = 4.65$ Å) and helically arranged along the 6_1 axis in such a way that the long axes of the octahedra avoid meeting at the same Cl atom. Since the Jahn–Teller energy gained by Cu^{2+} in an octahedral environment is high (1450 cm^{-1} $\cong$ 2100 K [11]), one has to assume that the $CuCl_6$ octahedra are also distorted in the high-temperature phase. The apparent high symmetry of this phase must, therefore, be brought about by averaging over a static or dynamic structural disorder.

Previous experiments [5, 6] have demonstrated that the disorder is dynamical. Phenomenologically, the disorder shows up in an intense diffuse scattering around the strong Bragg reflections and in an acoustic phonon anomaly connected with the c_{44} dispersion branch. The system could be modelled by assuming pseudo-spin phonon coupling

0953-8984/97/051067+11$19.50

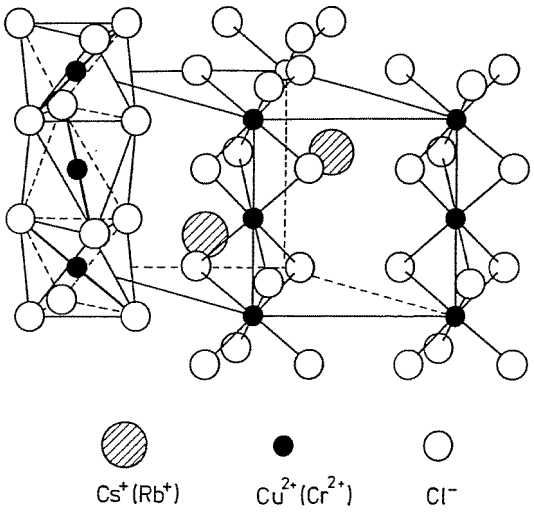

Figure 1. The structure of the high-temperature phase of $CsCuCl_3$, averaged over the dynamical disorder. The unit cell ($a = 7.227$ Å, $c = 6.15$ Å) contains two formula units. The space group is $P6_3/mmc$.

between reorientational jumps of the long octahedral axes and the acoustic (harmonic) lattice vibrations. Here, the pseudo-spin variable describes the orientation of the long octahedral axes with respect to the six crystallographically possible directions [7]. Recently, the theory was improved [8]. It describes very well the observed diffuse scattering and the c_{44} dispersion branch at higher q values. At smaller q values, the phonon signals seem to be overdamped. Only a few measurements with limited resolution have previously been made in this q regime. For very small q values the theory predicts the re-occurrence of sharp phonon signals shifted to drastically smaller energies. These renormalized phonons could not be verified in the previous experiments.

The present work concentrates on the small-q regime below 0.15 $Å^{-1}$ where the acoustic anomaly is most pronounced and the renormalized and overdamped phonons should occur. This range was systematically investigated as a function of temperature by high-resolution inelastic neutron scattering.

2. Experimental details

2.1. General details

The samples used were single crystals grown at room temperature from aqueous solution. Since the crystal quality of $CsCuCl_3$ deteriorates rapidly when cycling through the phase transition at 423 K, each sample was heated only once to the high-temperature phase. Consequently, different crystals were employed in different measuring periods. All crystals had a volume of about 2 cm^3 and mosaic spreads of 12–15 minutes of arc. The lattice constants at 434 K are $a = 7.227$ Å and $c = 6.151$ Å.

The temperatures investigated were room temperature and three temperatures above T_c: 424, 434 and 484 K. When measuring at 424 K (1 K above T_c), it was carefully checked that the superstructure reflections of the low-temperature phase had vanished.

Trying to balance resolution and intensity, three particular experimental set-ups were chosen to assess a small-, medium- and higher-phonon-wave-vector range. The measurements in the small-wave-vector range ($q = 0.01$–0.04 Å^{-1}) were carried out at the triple-axis spectrometer V2 installed at a cold-neutron guide of the reactor BER II of the Hahn-Meitner-Institut. The spectrometer was operated in a high-resolution set-up with constant $E_f = 3.0$ meV, horizontal collimations of open–20′–20′–20′, a beryllium filter in front of the sample, a vertically bent pyrolytic graphite monochromator and a flat pyrolytic graphite analyser. This configuration gives an elastic energy resolution of about 0.02 meV (full width at half maximum). The medium-wave-vector range ($q = 0.04$–0.1 Å^{-1}) was investigated at the same spectrometer with constant $E_f = 3.5$ meV and a more relaxed collimation of open–20′–20′–40′ leading to an energy resolution of about 0.03 meV. For the third wave-vector range ($q = 0.075$–0.15 Å^{-1}) the thermal triple-axis spectrometer E1 of the Hahn-Meitner-Institut was used with a constant $E_i = 13.7$ meV and horizontal collimations of 20′–10′–15′–20′. The spectrometer was equipped with a pyrolitic graphite monochromator and analyser, both vertically bent. The elastic energy resolution for this configuration is about 0.4 meV.

2.2. Measurements

Figure 2 shows constant-Q scans performed at $Q = (0.03\ 0\ 2)$, $Q = (0.06\ 0\ 2)$, and $Q = (0.10\ 0\ 2)$, which are representative for the three q ranges investigated. These scans probe transverse acoustic phonons of wave-vectors $q = 0.03$, $q = 0.06$, and $q = 0.1$ Å^{-1}, governed by the elastic constant c_{44}. The various temperatures at which the measurements were performed are denoted by particular symbols. One measurement below T_c is included in each plot for comparison. In all measurements above T_c a broad peak centred at $E = 0$ appears, which is much larger than the normal elastic incoherent peak visible in the measurements below T_c. This can clearly be seen in the measurements at small and medium q values. At high q values (measurementsat E1) the width of the zero-energy peak is mainly determined by the experimental resolution of about 0.4 meV (the intrinsic width of the zero-energy peak for $q = 0.1$ Å^{-1} is about 0.2 meV). This broad peak represents the quasi-elastic diffuse scattering predicted by the theory (‘dense’ Huang scattering [7]). At q values below 0.07 Å^{-1} (figures 2(a) and (b)) an additional sharp peak near $E = 0$ appears. It is indicated by the dashed lines, which represent Gaussian fits to the experimental data. This peak could be identified as a Bragg tail contamination. At very small q it can already be seen in the measurements below T_c (figure 2(a)). With increasing duration of the experiment, it becomes more and more prominent, since the mosaic width of the crystal is increasing, when keeping the sample at temperatures above T_c. Due to this contamination it was impossible to obtain meaningful results for q values less than 0.015 Å^{-1}, because there the phonon signals were completely hidden under the Bragg tail. At higher q values the Bragg tail was first subtracted from the experimental data, before they were further analysed.

The measurements above T_c show the following characteristics: the quasi-elastic diffuse scattering at $E = 0$ grows when approaching the phase transition temperature from above (see figure 2(c)); for q values of 0.015–0.05 Å^{-1} (see figure 2(a)) the phonon signals are strongly shifted towards smaller energies as compared to the corresponding measurements below T_c; in the q range 0.05 Å$< q <$ 0.09 Å^{-1} the phonons are strongly damped; at higher q values the phonon signals become sharper again with energies corresponding to the c_{44} value of the low-temperature phase.

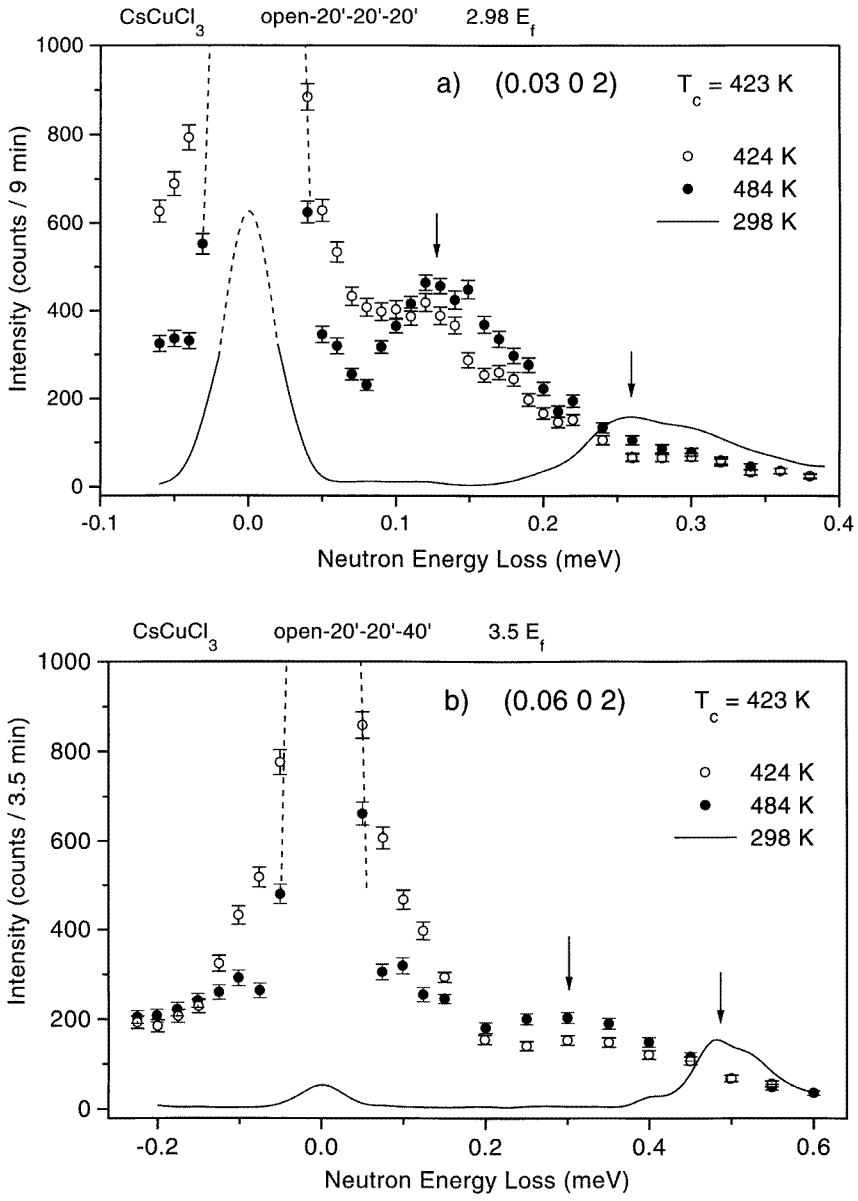

Figure 2. Constant-Q scans below and above T_c for (a) $Q = (0.03\ 0\ 2)$, (b) $Q = (0.06\ 0\ 2)$, and (c) $Q = (0.1\ 0\ 2)$. The symbols are explained in the insets. The dashed lines in (a) and (b) represent Gaussian fits to the Bragg tail contamination of the experimental data. The arrows indicate the phonon positions. Note the different energy scales.

Figure 3 gives an overview of the phonon positions in q, E space, obtained by fitting Gaussians to the measured phonon signals. The open symbols denote measurements performed below T_c and the full symbols represent the measurements above T_c. Different symbols characterize the different q ranges investigated by different experimental set-ups.

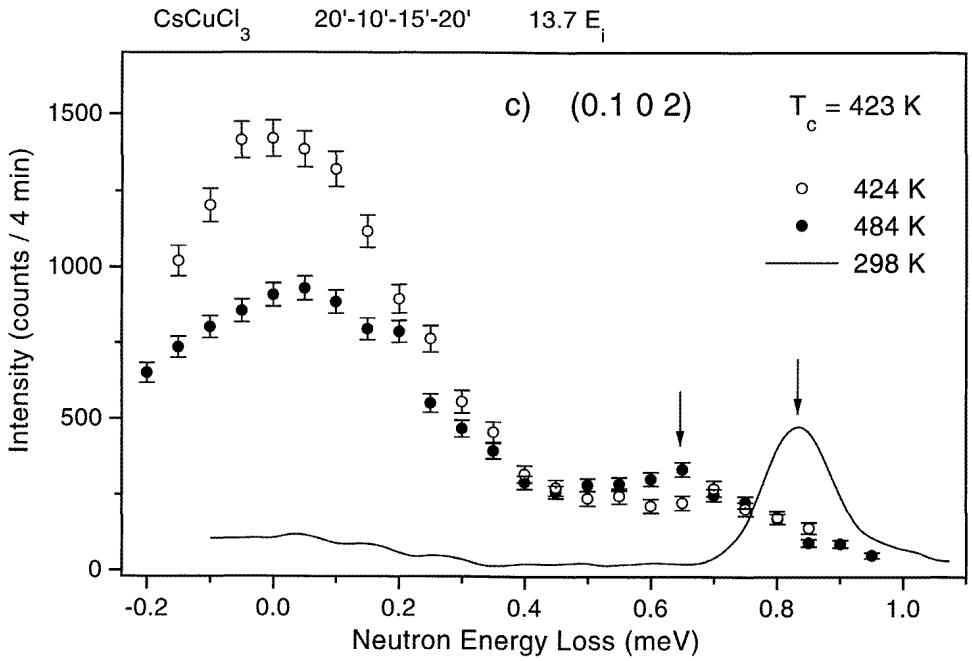

Figure 2. (Continued)

At q values greater than 0.1 Å^{-1} the dispersion curve above T_c follows closely the dispersion curve below T_c. At small q values up to 0.05 Å^{-1}, however, the high-temperature dispersion curve is very flat. Its slope corresponds to the sound velocity measured by Lüthi (quoted in [1]). In the intermediate-q regime, where the phonon signals are strongly damped, a transition between the flat and the steep part of the dispersion curve occurs.

3. Theoretical background

Based on the pseudo-spin phonon coupling theory of Yamada *et al* [9], Schotte *et al* [7, 8] have developed a theory to describe the observed phenomena in the high-temperature phase of $CsCuCl_3$ and related compounds: the distorted octahedra are modelled by elastic dipoles, which randomly occupy the six possible orientations in the hexagonal unit cell of the high-temperature phase. A particular orientation is described by a pseudo-spin variable and a relaxator *ansatz* is made for the reorientation dynamics. In the following the results of [8] will be applied.

The inelastic scattering function can be written as

$$S(\boldsymbol{K},\omega) = |F_{hkl}|^2 \sum_{ij} (\boldsymbol{K}\cdot\boldsymbol{e}_i)(\boldsymbol{K}\cdot\boldsymbol{e}_j)\langle Q_i Q_j\rangle_\omega \qquad i,h = 1,2,3 \tag{1}$$

where F_{hkl} denotes the structure factor including the Debye–Waller factor. $\boldsymbol{K}$ is the scattering vector, $\boldsymbol{e}_i$ and $\boldsymbol{e}_j$ are the normalized polarization vectors of a lattice wave with wave-vector $\boldsymbol{q}$ and Q_i and Q_j are the phonon amplitudes of the three normal modes. For

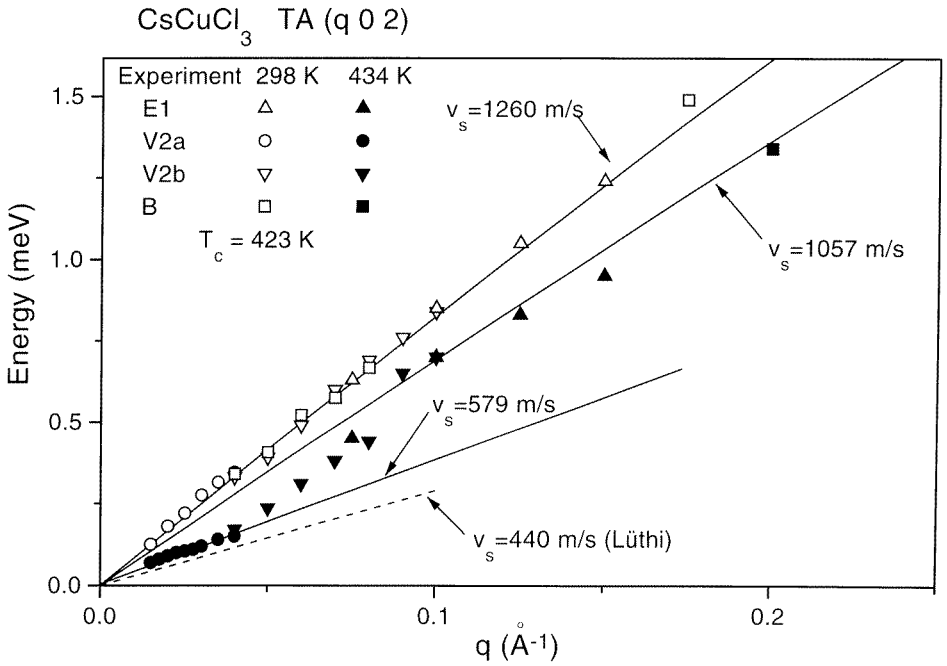

Figure 3. Dispersion curves for the TA phonons measured at (q 0 2) below and above T_c (open and full symbols respectively). The various labels denote different experiments: E1, spectrometer E1 (Berlin) with $E_i = 13.7$ meV; V2a, spectrometer V2 (Berlin) with $E_f = 3.0$ meV; V2b, spectrometer V2 (Berlin) with $E_f = 3.5$ meV; B, previously measured data (Brookhaven [6]). The long solid lines represent sine curves fitted to the peak positions of the phonon signals at higher q values. The short solid line is fitted to the peak positions of the soft phonons at small q values. The corresponding sound velocities v_s are given in the figure. The short dashed line represents a sound velocity measurement above T_c by Lüthi. It fits to the dispersion of the renormalized phonons at very small q.

the special case of $\boldsymbol{K} = (q\ 0\ l)$ in good approximation the leading contribution is from $\boldsymbol{e}_i = \boldsymbol{e}_j = \boldsymbol{e}_1 = (0\ 0\ 1)$:

$$\langle Q_1 Q_1 \rangle = \frac{kT}{\pi\gamma}\frac{h^2(\boldsymbol{q})}{kT}(\omega^2-\omega_2^2)(\omega^2-\omega_3^2)^2\Bigg[\prod_i\left(\omega^2-\omega_i^2+\frac{h_i^2(\boldsymbol{q})}{kT}\right)^2 + \frac{\omega^2}{\gamma^2}\prod_i(\omega^2-\omega_i^2)^2\Bigg]^{-1} \qquad i=1,2,3 \tag{2}$$

with γ as the undisturbed relaxation rate of the pseudo-spins, k the Boltzmann constant, and T the temperature. Here, in contrast to [7], a factor $6kT$ is included in the definition of γ. The undisturbed ('hard') phonon frequencies are given by the frequencies ω_i of the three normal modes, the soft frequencies by $\omega_i^2 - h_i^2(\boldsymbol{q})/kT.h_j$ describes the pseudo-spin phonon coupling:

$$h_i^2 = \frac{1}{6}\sum_{r=1}^{6}(\mathbf{P}^r\boldsymbol{q}\cdot\boldsymbol{e}_i)^2 \tag{3}$$

The tensors $\mathbf{P}^r$ represent the elastic dipoles [7]:

$$\mathbf{P}^r = -V_D \frac{\Delta d}{d}\left[c_{66}\begin{pmatrix} P^r_{xx} & P^r_{xy} & 0 \\ P^r_{xy} & P^r_{yy} & 0 \\ 0 & 0 & 0 \end{pmatrix} + c_{44}\begin{pmatrix} 0 & 0 & P^r_{xz} \\ 0 & 0 & P^r_{yz} \\ P^r_{xz} & P^r_{zy} & 0 \end{pmatrix}\right]. \tag{4}$$

Here, the $P^r_{xx} \ldots P^r_{zy}$ are components (simple numerical factors) of rotation matrices describing the orientation of the octahedra in the crystal lattice; c_{66} and c_{44} are the undisturbed ('hard') elastic constants, V_D refers to an effective volume of the elastic dipole and $\Delta d/d$ describes the elongation of the octahedron, with Δd being the difference between the short and the long axis and d the average axis length (for details see [6, 7]).

The rate Γ of the reorientational jumps of the long octahedral axes is related to the relaxation parameter γ by

$$\Gamma = \gamma \prod_i \left(\omega_i^2 - \frac{h_i^2}{kT}\right)\left(\prod_i \omega_i^2\right)^{-1}. \tag{5}$$

This expression can be derived from (2) for $\omega \to 0$ at large q. Under these conditions the peak at $E = 0$ has a Lorentzian shape of width Γ.

Table 1. Parameters obtained by fitting the theoretical curve convoluted with the experimental resolution to the measurements in the high-temperature phase. In parentheses are the standard deviations in units of the last digit. The parameters are explained in the text. Note that the relaxation rate γ is given on the energy scale (meV), which can be converted to hertz by multiplying by 4.14×10^{12} J^{-1} s^{-1}. The reliability coefficient R describes the quality of the fit and is given by $R = 100[\chi^2/\Sigma(I_i/\sigma_i)^2]^{1/2}$ (I_i, observed intensity; σ_i, standard deviation; χ^2, sum over the squared deviations weighted by the σ_i).

	424 K	434 K	484 K
c_{11} (10^{10} dyn cm^{-2})	29.1 (fixed)	29.1 (fixed)	29.1 (fixed)
c_{66} (10^{10} dyn cm^{-2})	8.23 (fixed)	8.23 (fixed)	8.23 (fixed)
c_{44} (10^{10} dyn cm^{-2})	5.35 (fixed)	5.34(6)	5.39(7)
γ (meV)	1.25(2)	1.26(2)	1.77(3)
A_{JT} (10^{-10} cm^2 dyn^{-1})	0.1506(2)	0.148(1)	0.143(1)
R	16.9	17.4	19.5

4. Results and discussion

The measured data were analysed using the theoretical scattering function of (1) and (2) convoluted with the experimental resolution. Only the $\langle Q_1 Q_1 \rangle$ term was considered, since contributions from other $\langle Q_i Q_j \rangle$ combinations are numerically mall for the $(q\ 0\ l)$ directions. The scattering function was parametrized in such a way that a scale factor for each data batch, the undisturbed elastic constants c_{11}, c_{44}, and c_{66}, the undisturbed relaxation rate γ, and a factor A_{JT} were free variables. A_{JT} is basically the prefactor in front of the brackets of (4). It describes the 'dipole strength' and is defined as $A_{JT} = (\rho/mkT)(V_D \Delta d/d)^2$ with ρ the density and m the mean reduced mass of an atom in the lattice as given by

$$m^{-1} = 0.2m_{Cs}^{-1} + 0.2m_{Cu}^{-1} + 0.6m_{Cl}^{-1}.$$

All data obtained for a particular temperature, but for different q values, were fitted jointly (see figures 4–6). For this procedure, the q range at each temperature was enlarged by adding a small number of data previously measured [6] at very high q values. The results

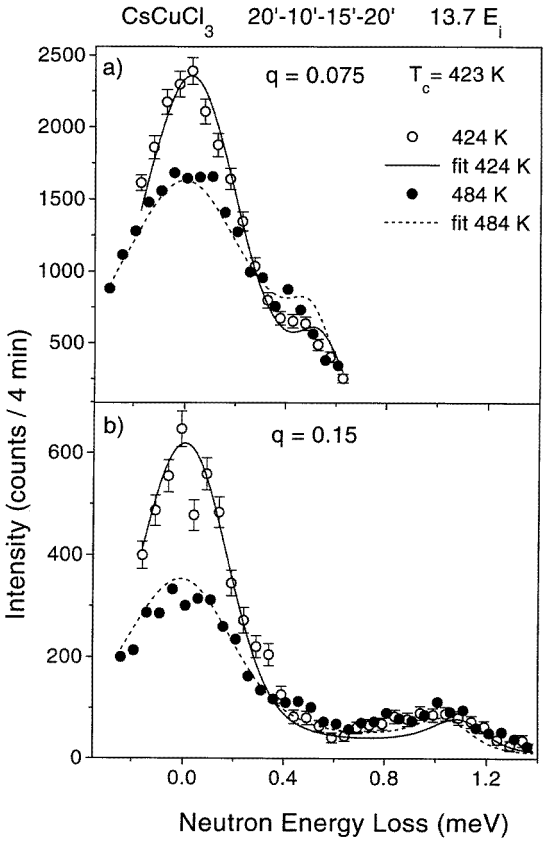

Figure 4. A comparison between experiment and theory for constant-Q scans at $Q = (q\ 0\ 2)$ with (a) $q = 0.075$ and (b) $q = 0.15$. The calculated curves for the two temperatures are given by the solid and the dashed line.

are listed in table 1. Since the fit was not stable with all parameters free at the same time, c_{11}, c_{66}, and also c_{44} in the case of the 424 K data were kept fixed at the values 29.1, 8.23, and 5.35 respectively. These values were found when fitting the previously measured data [6] with the improved theory [8]. The parameter c_{44} is strongly correlated with A_{JT}. For the data measured at higher temperatures, however, an independent fit of c_{44} together with the other parameters γ and A_{JT} was possible. The values obtained for the undisturbed elastic constants are in good agreement with the values of 28.96, 8.84, and 5.49×10^{10} dyn cm^{-2} found by Soboleva *et al* [10] for the low-temperature phase by ultrasonic measurements. The elastic constants do not change conspicuously within the temperature range investigated.

The parameter A_{JT} is inversely temperature dependent, as expected from its definition given above. Its value is a factor of 1.6 higher in the present work than found previously [6]. This is a consequence of the improvement of the theory. A similar value for A_{JT} is obtained when analysing the previously measured data with the improved theory. The higher value for A_{JT} is physically more plausible. As shown in [6], the parameter A_{JT} combined with the elastic constants c_{44} or c_{66} can be related to the Jahn–Teller energy E_{JT} of a $CuCl_6$ octahedron: $E_{JT} \approx c_{44} V_D \Delta d/d \approx \sqrt{2c_{66}} V_D \Delta d/2d$. Using the parameters obtained in the present fit, E_{JT} is calculated to be 1180 and 1280 cm^{-1} for c_{44} and c_{66},

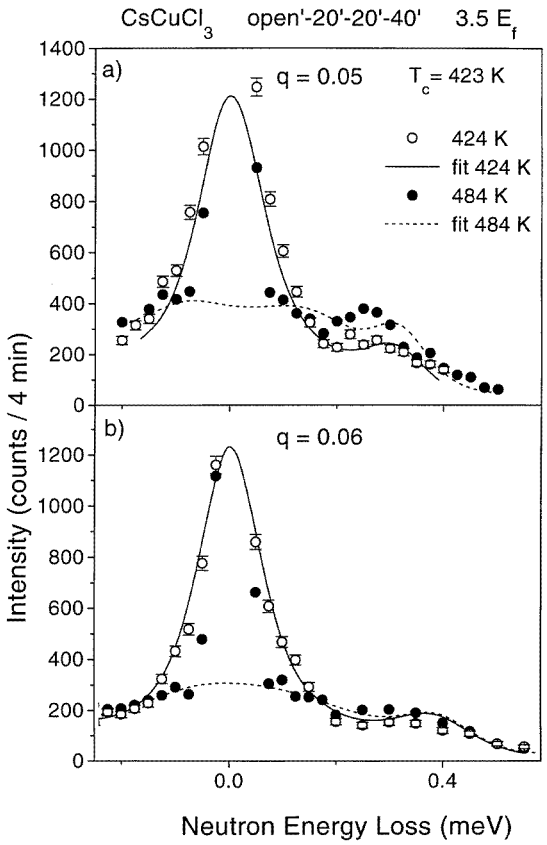

Figure 5. A comparison between experiment and theory for constant-Q scans at $Q = (q\ 0\ 2)$ with (a) $q = 0.05$ and (b) $q = 0.06$. Data and calculated curves for two different temperatures are shown.

respectively. This is in much better agreement with the value of 1450 cm^{-1} given by Reinen and Friebel [11] than the values of 740 and 1000 cm^{-1} found in the previous work. According to the definition of A_{JT} given above, A_{JT} can also be interpreted geometrically. Assuming $\Delta d/d = 0.19$, the value of the low-temperature structural data [12], the effective dipole volume V_D for the three temperatures is calculated to be 22.7, 22.8, and 23.7 $Å^3$. This volume corresponds to a perfect octahedron of an axis length of 5 Å, which is close to the value of 4.9 Å, the average axis length derived from the structural data.

For the relaxation parameter γ an Arrhenius type dependence on temperature can be expected. The values obtained in the present work point to such a temperature dependence, but the small number of different temperatures investigated does not allow a more detailed analysis. From γ the physically meaningful jumping rate Γ can be deduced according to (5). The value obtained for $T = 424$ K is $\Gamma \approx 2 \times 10^{10}$ Hz $\cong 0.1$ meV. This is the same value as previously found [6].

Figures 4–6 show the experimental data together with the theoretical curves from which the parameters of table 1 were obtained for various q values and temperatures. As shown in figure 4, the calculated curves agree very well with the measured data at the higher q values. The phonon signals and the quasi-elastic diffuse peaks are excellently modelled by the

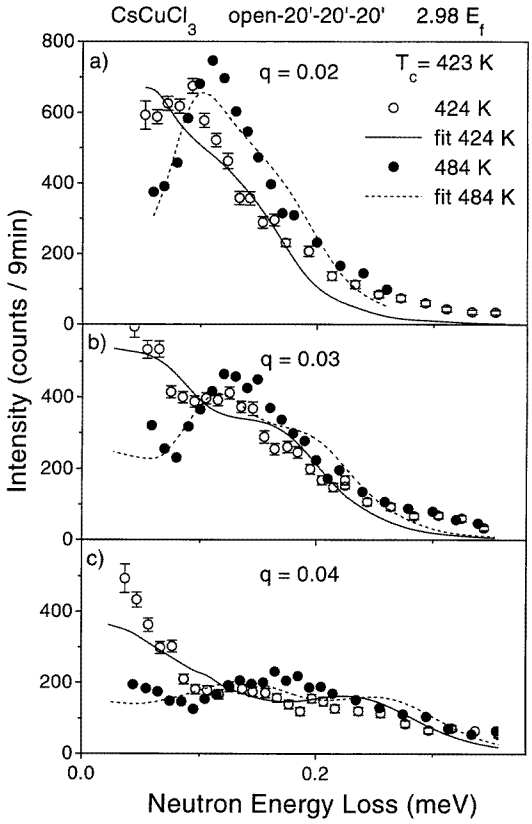

Figure 6. A comparison between experiment and theory for constant-Q scans at $Q = (q\ 0\ 2)$ with (a) $q = 0.02$, (b) $q = 0.03$, and (c) $q = 0.04$. Data and calculated curves for two different temperatures are shown.

theory. The theoretical curves also describe the temperature dependence of the quasi-elastic diffuse scattering correctly. For the small q values, shown in figure 5, the agreement is less perfect. It is reasonable for the renormalized phonons at very small q (figure 6(a)). The temperature shift towards higher energies is well reproduced by the theoretical curve. The agreement becomes worse, however, when approaching the regime of the damped phonons (figure 6(c)). For these small q values the quasi-elastic diffuse scattering could not be compared with the theory, because of the Bragg tail contamination in the experimental data.

5. Summary

The present work has demonstrated that the distinct predictions of the pseudo-spin phonon coupling theory for the small-q phonons in the high-temperature phase of $CsCuCl_3$ are essentially correct: the appearance of renormalized phonons could for the first time be confirmed by experiment. Including the results of the previous work one can say that the theory describes very well the neutron scattering experiments in the dynamically disordered high-temperature phase of $CsCuCl_3$ over a large wave-vector, energy and temperature range. The elastic constants and A_{JT}, parameters used in the theory, are refined to physically

meaningful values in the fits. The relaxation rate γ is basically the only parameter without a further cross check by other observations.

References

[1] Hirotsu S 1977 *J. Phys. C: Solid State Phys.* **10** 967
[2] Crama W J and Maaskant W J A 1983 *Physica* B **121** 219
[3] Tanaka H, Dachs H, Iio K and Nagata K 1986 *J. Phys. C: Solid State Phys.* **19** 4861
[4] Tanaka H, Dachs H, Iio K and Nagata K 1986 *J. Phys. C: Solid State Phys.* **19** 4879
[5] Graf H A, Tanaka H, Dachs H, Pyka N, Schotte U and Shirane G 1986 *Solid State Commun.* **57** 469
[6] Graf H A, Shirane G, Schotte U, Dachs H, Pyka N and Iizumi M 1989 *J. Phys.: Condens. Matter* **1** 3743
[7] Schotte U, Graf H A and Dachs H 1989 *J. Phys.: Condens. Matter* **1** 3765
[8] Schotte U, Kabs M, Dachs H and Schotte K D 1992 *J. Phys.: Condens. Matter* **4** 9283
[9] Yamada Y, Takatera H and Huber D L 1974 *J. Phys. Soc. Japan* **36** 641
[10] Soboleva L V, Sil'vestrova I M, Perekalina Z B, Gil'varg A B and Martyshev Y N 1976 *Sov. Phys-Crystallogr.* **21** 660
[11] Reinen D and Friebel C 1979 *Structure and Bonding* vol 37 (Berlin: Springer)
[12] Crama W J 1980 *Thesis* University of Leiden